Pandanus Conoideus Lamk Protects Inflammation by Regulating Reactive Oxygen Species and Nuclear Factor Kappa B in Lps-Induced Murine Macrophages

Yun-Hee Rhee[1], Ye Kyu Park[2], Tae-Hong Park[3] and Jong-Soo Kim[2]*

[1]Laser Translational Clinical Trial Center, Dankook University Hospital, Republic of Korea

[2]Departments of Obstetrics and Gynecology, College of Medicine, Dankook University, Republic of Korea

[3]Smile International Co. Ltd., Republic of Korea

Submission: April 09, 2020; **Published:** May 13, 2020

*Corresponding author: Jong-Soo Kim, Departments of Obstetrics and Gynecology, College of Medicine, Dankook University, Cheonan, Republic of Korea.

Abstract

Background: Pandanus conoideus Lamk (Red fruit) is a Papuan traditional food which has been used to treat various diseases. Despite these various effects of Red fruit, little is known about the physiological mechanism.

Aims: The aim of this study was to investigate the anti-inflammatory properties of Red fruit oil (RFO) and establish the signal pathway of leading compounds.

Methods: Raw 264.7 murine macrophage cells were used with lipopolysaccharide (LPS). Cell viability and the pro-inflammatory factors were investigated using MTT assay, real time PCR, western blot analysis, and Enzyme linked immuno-sorbent assay (ELISA). The quantification of leading compounds in RFO was performed using high performance liquid chromatography (HPLC).

Results: RFO did not affect cell viability. RFO significantly reduced the production of nitric oxide (NO) and prostaglandin E2 (PGE2), and both the protein level and mRNA level of iNOS in LPS-induced macrophages. RFO also regulated the reactive oxygen species (ROS) in LPS-induced macrophages. RFO attenuated the translocation of NF-κB p65 subunit, phosphorylation of I-κB, extracellular signal-regulated kinase (ERK), and c-Jun N-terminal kinase (JNK) in a dose-dependent manner. HPLC analysis determined that 1 g of RFO had 14.05±0.8 mg of β-cryptoxanthin and 7.4±0.7 mg of β-carotene.

Conclusion: RFO provides an anti-inflammatory effect by regulating ROS and NF-κB through MAPK due to the antioxidant activity.

Keywords: Pandanus conoideus Lamk; Macrophages; Anti-inflammation; ROS; NF-κB; β-cryptoxanthin

Abbreviations: RFO: Red fruit (Pandanus conoideus Lamk) oil; LPS: Lipopolysaccharide; NO: Nitric oxide; iNOS: Inducible NO synthase; IL: Interleukin; ROS: Reactive oxygen species; ELISA: Enzyme linked immuno-sorbent assay; HPLC: High performance liquid chromatography; COX-2: Cyclooxygenase-2; PGE2: Prostaglandin E2; ERK: Extracellular signal-regulated kinase; JNK: c-Jun N-terminal kinase; MAPK: Mitogen-activated protein kinase; DMEM: Dulbecco's modified Eagle medium; FBS: Fetal bovine serum; DCFH-DA: 2'7'-dichlorofluorescein diacetate; MTT: 3-(4,5-dimethylthiazol-2-yl)-2,5-diphenyltetrazolium bromide; RT- PCR: Real time polymerase chain reaction

Introduction

The inflammation process is tightly regulated by both initiation and maintenance signals and considered to be a major risk factor in the pathogenesis of chronic diseases where the macrophages are important immune cells which regulate inflammation producing expression of inflammatory proteins and pro-inflammatory chemokines, cytokines, and nitric oxide (NO) [1,2]. Macrophages are highly sensitive to initiators of inflammation as lipopolysaccharide (LPS) which respond by the release of mediators not only interleukins (ILs) and cytokines, but also inducible NO synthase (iNOS) and reactive oxygen species (ROS), which inducing the inflammatory gene expression where each is associated somehow with the pathophysiological of the

inflammation [3-5]. Because macrophages produce a wide range of biologically active molecules participated in both beneficial and detrimental outcomes in inflammation, modulation of macrophage activation is a good strategy to prevent this diseases. Red fruit (Pandanus conoideus Lamk) is Papuan traditional food which has been used to treat various diseases such as cancer [6] preeclampsia [7], hepatitis [8], liver cirrhosis [9], diabetes mellitus [10], and sinusitis [11]. This bioavailability of red fruit has been due to unsaturated fatty acids such as palmitoleic acid, oleic acid, linoleic acid, linolenic acid and some carotenoids [10,12]. Despite these many biological effects, few researches were reported on the mechanism of red fruit oil (RFO). β-cryptoxanthin is a typical carotenoid found abundantly in persimmon, papaya, paprika, and carrot. β-cryptoxanthin has been reported to possess several beneficial functions, such as antioxidant, cancer-preventive effects, and anti-metabolic syndrome effects [13-16]. In present study, we hypothesized that the cause of this anti-chronic inflammation and anti-cancer effect is due to antioxidant function of RFO, and evaluated the anti-inflammatory effect of RFO on LPS-stimulated RAW 264.7 macrophage cells. We also investigated the mechanism of inflammatory effect of reduced ROS by RFO in LPS-stimulated macrophages and investigated the component of β-cryptoxanthin in RFO.

Materials and Methods

Chemicals and reagents

RFO (APOTEK®) was supplied from Smile international Co., Ltd (Seoul, Korea). Dulbecco's modified Eagle medium (DMEM), fetal bovine serum (FBS), and penicillin–streptomycin was purchased from Corning (Oneonta, NY, USA). 2'7'-dichlorofluorescein diacetate (DCFH-DA) and anti-iNOS antibody were purchased from BD (San Jose, CA, USA). Peroxidase-conjugated secondary antibodies and TriZol were purchased from Life technologies (Grand island, NY, USA). Phosphor-JNK, phosphor-ERK, phosphor-p38, phosphor-IκB and NF-κB antibodies were purchased from Cell Signaling Technology Inc. (Beverly, MA, USA). The enzyme immunoassay kit used for prostagladin E$_2$ (PGE2) was obtained from R&D Systems (Minneapolis, MN, USA). The ECL detection reagents were purchased from GE Healthcare (Buckinghamshire, UK). LPS (Escherichia coli 0111: B5) was purchased from Creative Biolabs (Shirley, NY, USA). β-actin, 3-(4,5-dimethylthiazol-2-yl)-2,5-diphenyltetrazolium bromide (MTT), and other chemicals were purchased from Sigma–Aldrich (St. Louis, MO, USA).

Cell culture

RAW 264.7, the murine macrophage cell line was purchased from American Type Culture Collection and maintained in DMEM supplement with 1 mg/mL glucose, 10% FBS, 100 mg/mL penicillin-streptomycin at 37 °C with 5% CO$_2$.

Cell viability assay

The cytotoxic effect of RFO against RAW264.7 cell lines was evaluated by MTT assay. Briefly, cells were seeded at a density of 5×10^3 cells/well in a 96-well plate for 24 h. Then, the cells were treated with at various concentrations of fractions with or without 1 μg/mL LPS. After 24 h, 2 mg/mL MTT was added onto each well, then incubated until formazan was constituted for 3h. The formazan was dissolved in dimethyl sulfoxide (DMSO) and the absorbance at 550 nm was measured using microplate reader (Molecular Devices, Sunnyvale, CA). Cell viability was calculated as a percentage of viable cells in drugs treated group versus untreated control. Each experiment was repeated three times.

Nitrite assay

Cells were treated with various concentrations of RFO for 30 min and incubated with 1 μg/mL LPS for 24 h. Because NO production is reflected in the accumulation of nitrite in the cell culture medium, 50 μL of supernatants were removed and mixed with the same volume of Greiss reagent (Promega, Madison, WI). After incubation for 10 min, the absorbance of mixture at 450 nm was measured using a spectrophotometer (TECAN, Austria). The nitrite levels were estimated as the percentage of absorbance of the sample to the respective controls.

Cyclooxygenase2 (COX-2) assay

Cells were treated with various concentrations of RFO for 30 min and incubated with 1 μg/mL LPS for 24 h. After incubation, the supernatants were removed and followed COX-2 measurement. The COX-2 concentrations were evaluated using a specific enzyme immunoassay (EIA) kit (Cayman, Ann Arbor, MI) according to the manufacturer's instructions.

Prostaglandin E2 assay

Cells were treated with various concentrations of RFO for 30 min and incubated with 1 μg/mL LPS for 24 h. After incubation, the supernatants were removed and followed PGE$_2$ measurement. The PGE$_2$ concentrations were evaluated using a specific enzyme immunoassay (EIA) kit (Cayman, Ann Arbor, MI) according to the manufacturer's instructions.

iNOS gene measurement by real-time PCR

The cells from the supernatants had been removed were subjected to RNA isolation. RNA isolation was performed using TRIzol reagent according to the manufacturer's instructions. cDNA was synthesized using hyperscript RT master mix (GeneAll, Daejeon, Korea). The primers were described as; iNOS forward: 5'-ATGTCCGAAGCAAACATCAC-3', reverse: 5'-TAATGTCCAGGAAGTAGGTG-3', and GAPDH forward: 5'-TGTGATGGTGGGAATGGGTCAG-3', reverse: 5'-TTTGATGTCAC GCACGATTTCC-3'. The PCR was amplified using ABI 7500 and Taqman gene expression master mix (Applied Biosystems, Waltham, MA, USA). The quantitative analysis was performed to compare the $\Delta\Delta$Ct after the normalization by GAPDH as an internal control. After analysis, PCR products were electrophoresed on 3% agrose gel and images were taken by cybergreen detection using Kodak imagestation FX® (Kodak, Rochester, NY, USA)

Analysis of ROS by flowcytometry

Cells were treated with various concentrations of RFO for 30 min and incubated with 1 μg/mL LPS for 24 h. Cells were followed by the addition of 10 mg/mL DCFH-DA. The suspensions were washed with PBS after incubation for 20 min. The suspensions were then assayed with a flowcytometer (C6 Accuri, BD, Bedford, MA, USA) according to Rhee et al. [4].

Western blot analysis

Cells were treated as described previously, then total lysates were prepared with lysis buffer (50 mM Tris (pH 7.4), 300 mM NaCl, 5 mM EDTA (pH 8.0), 0.5 % Triton X-100, 1 mM aprotinin, 1 mM leupeptin, 1mM pepstatin, 10mM iodoacetamide, and 2 mM phenylmethylsulfonyl fluoride (PMSF). Meanwhile, each nucleus extracts and cytosol extracts were isolated using a NE-PER nuclear and cytoplasmic extraction reagent kit (Pierce, Rockford, IL). Briefly, cells were washed with PBS, and were prepared with ice-cold extraction buffers sequentially. After centrifugation at 16,000xg, the cytoplasmic protein and nuclear extract were separated. Total lysates and nuclear fractions were estimated with Bio-Rad dye reagent concentrate (Bio-Rad Laboratories, Hercules, CA), then resolved on a 10% SDS-PAGE. After electrophoresis, the proteins were electro transferred to a PVDF membrane, blocked with 1% BSA, and probed with anti-iNOS (1:1,000), phospho-JNK (1:1,000), phospho-ERK (1:1,000), phospho-p38 (1:1,000), phospho-IκB (1:1,000), and NF-κB (1:500) antibodies at 4 °C overnight. The blot was washed, exposed to HRP-conjugated secondary antibodies for 2 h, and finally developed through enhanced chemiluminescence. For ß-actin detection, previously used membranes were soaked in stripping buffer (62.5 mM Tris-HCl, pH 6.8, 150 mM NaCl, 2% SDS, 100 mM ß-mercaptoethanol) at 65 °C for 30 min and hybridized with anti-ß-actin. The relative protein expression was densitometerically quantified using the BioRad GS-670 densitometer (BioRad, Hercules, CA) and normalized to β-actin.

High performance liquid chromatography (HPLC)

To determine the content of β-cryptoxanthin in RFO, we performed HPLC analysis according to previous studies [17]. HPLC analysis was performed using Agilent 1100 model with a pump (G1311C), auto sampler (G1329B), column, and diode array detector purchased from Agilent (Santa Clara, CA, USA). The analysis conditions are described in Table 1.

Table 1: HPLC analysis conditions.

Detector	Diode array detector
Wavelength	474nm
Column	YMC C30® carotenoid column (250 × 4.6 mm, 9μm)
Mobile phase	Methanol: MTBE: 0.1% H_3PO_4 = 16:80:4
Running time	35min

Flow rate	0.9mL/min
Injection volume	120ㅣ
Temperature	25 ℃

Statistical analysis

All results are presented as mean ± S.D. and are representing three or more independent experiments. Data were compared using the one-way ANOVA using Prism® (GraphPad, La Jolla, CA, USA) with p-values less than 0.05 considered statistically significant.

Results

RFO did not affect cell viability

Figure 1A showed the effect of RFO on viability of RAW 264.7 with or without LPS. Cell viability was not affected against 10-1,000 μg/mL of RFO with or without LPS.

RFO reduced NO in LPS-induced macrophages

To assess the effects of RFO on NO production in LPS-induced RAW 264.7 macrophages, cells were treated with various concentrations of RFO for 30 min, then incubated with 1 μg/mL LPS for 24 h. NO release was elevated 224 ± 19.24% (p < 0.001) following LPS treatment, which was reduced 224 ± 19.24% at 10 μg/mL (p < 0.05), 161.38 ± 21.81% at 25 μg/mL (p < 0.001), and 136.16 ± 30.56% at 50 μg/mL (p < 0.001) with RFO combination (Figure 1B).

RFO decreased COX-2 production in LPS-induced macrophages

COX-2 production was significantly increased from 33.17 ± 5.23 ng/mL to 86.25 ± 1.88 ng/mL (p < 0.001) following LPS treatment. However, it was reduced 60.52 ± 12.49 ng/mL at 10 μg/mL (p < 0.05), 32.16 ± 8.85 pg/mL at 25 μg/mL (p < 0.001), and 13.27 ± 1.67 ng/mL at 50 μg/mL (p < 0.001) with RFO combination (Figure 1C).

### RFO also decreased PGE2 production in LPS-induced macrophages

Meanwhile, PGE2 production was significantly increased 440.6 ± 35.36 pg/mL (p < 0.001) following LPS treatment, which was reduced 227.5 ± 13.6 pg/mL at 10 μg/mL (p < 0.001), 180.77 ± 48.95 pg/mL at 25 μg/mL (p < 0.001), and 103.27 ± 51.67 pg/mL at 50 μg/mL (p < 0.001) with RFO combination (Figure 1D).

RFO suppressed both mRNA and protein levels of iNOS in LPS-induced macrophages

To determine the inhibitory effects of RFO on pro-inflammatory mediator NO, COX-2, and PGE2 production, the biosynthesis of transcriptional levels of iNOS was performed with semi-quantitative reverse-transcription PCR and western blot analysis on LPS-induced RAW 264.7 macrophages. Figure

1D indicates that both mRNA level and protein level of iNOS were significantly decreased by treatment of RFO (p < 0.001). Consistent with the findings shown in Figure 1E, RFO had a significant concentration-dependent inhibitory effect on the inflammation through pro-inflammatory mediator NO in LPS-induced RAW 264.7 macrophages.
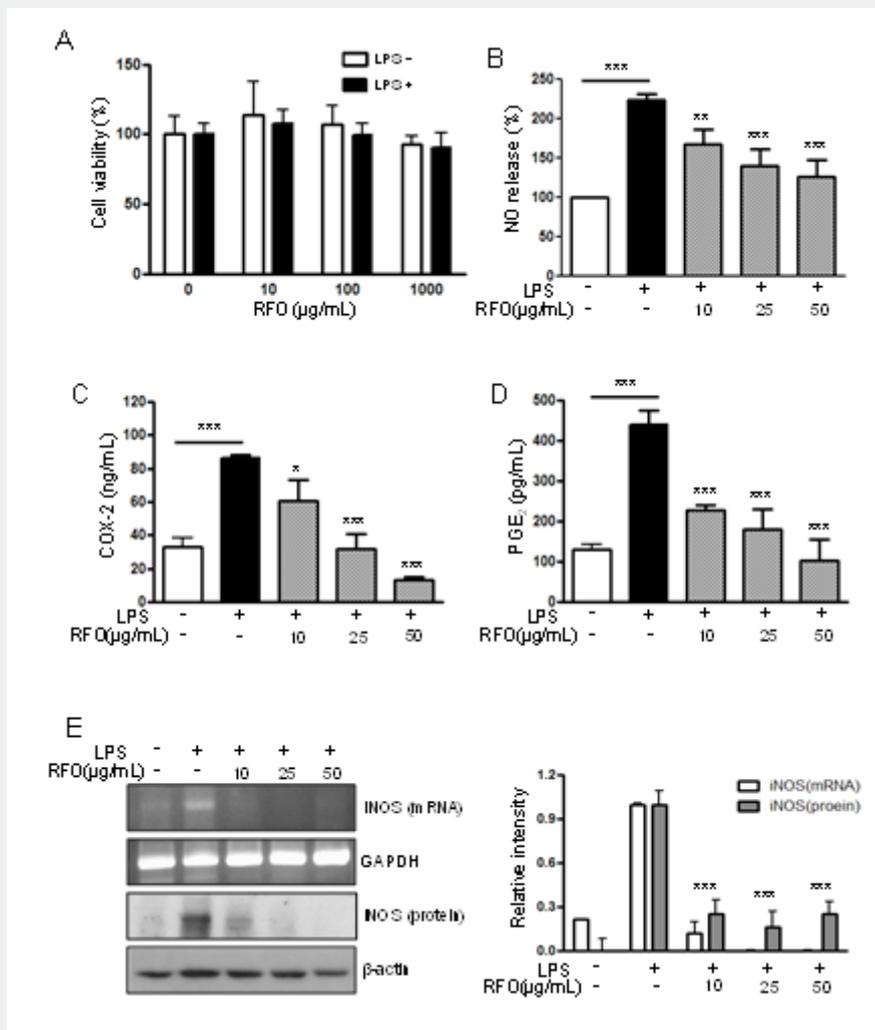

Figure 1: Effect of RFO on cell viability, NO release, PGE2 production, protein level of iNOS, and mRNA level of iNOS in LPS-induced RAW 264.7 cells.

The cytotoxic effect of all fractions from RFO against RAW 264.7 cell lines was evaluated by MTT assay. Cell viability was calculated as a percentage of viable cells in drugs treated group versus untreated control. The data are represented as the mean±S.D. (n=6) of three independent experiments (A). The cells were incubated with 10-50 μg/mL of RFO in the presence or absence of LPS (1 μg/mL) for 24 h. The percentage of NO release (B), the production of COX-2 (C), the production of PGE2 (D), and mRNA and protein levels of iNOS (E) were evlauated. Quantification of iNOS levels are expressed as the ratio of iNOS/GAPDH in PCR assay or iNOS/β-actin in western blot analysis; The results from replication are expressed as the mean±S.D. (n=3). **p<0.05 and ***P<0.001 compared with the LPS group.

RFO attenuated ROS in LPS-induced macrophages

The excess ROS is known to be injured intracellular proteins, lipids and nucleic acids and induce inflammation [18]. Thus, we investigated the ROS production in response to LPS using flowcytometry. DCFH-DA binds ROS produced cells. Figure 2 showed the DCFH-DA positive cells were increased following LPS treatment from 40.71 ± 2.11% to 70.87 ± 3.09%. However, ROS production was also significantly inhibited by RFO with a dose dependent manner; 47.08 ± 2.45% at 10 μg/mL (p < 0.001), 41.34 ± 1.41% at 25 μg/mL (p < 0.001), and 33.76 ± 3.56% at 50 μg/mL (p < 0.001).
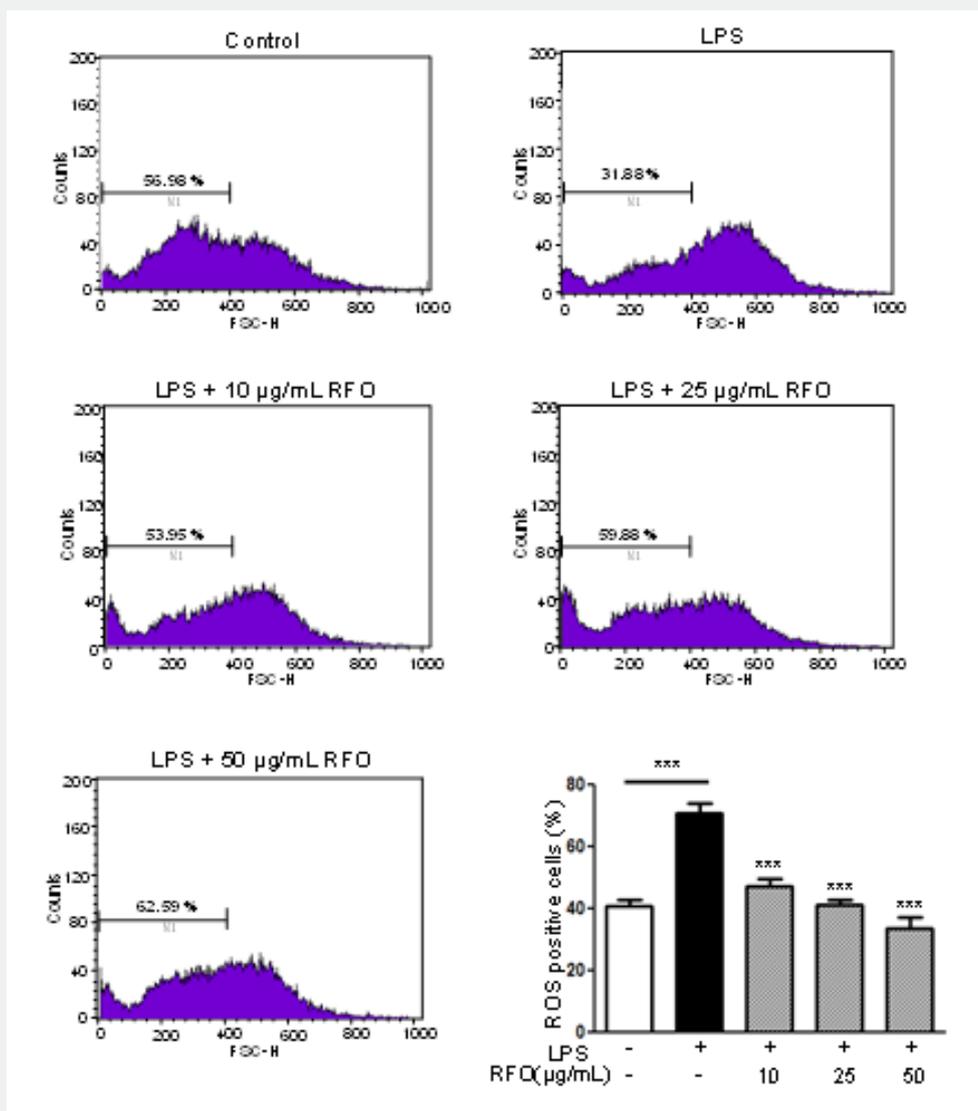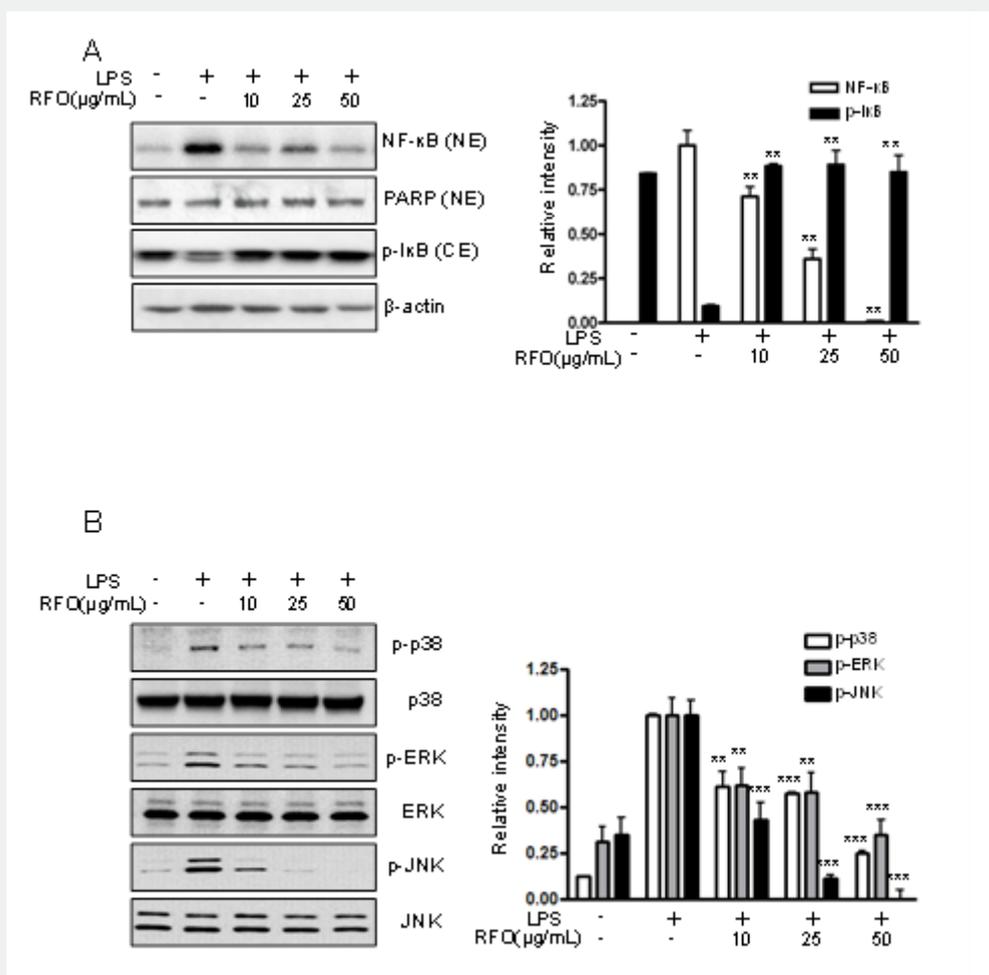
Figure 2: Effect of RFO on and ROS in LPS-induced RAW 264.7 cells.

The cells were incubated with 10-50 µg/mL of various fractions in the presence or absence of LPS (1 µg/mL) for 24 h. The cells were pre-incubated for 1 h in the presence or absence of LPS before the addition of RFO fractions, followed by the addition of 10 □g/mL 2'7'-dichlorofluorescein diacetate (DCFH-DA). The results from replication are expressed as the mean±S.D. (n=3). ***P<0.001 compared with the LPS group.

RFO suppressed nuclear translocation of the NF-κB p65 subunit via MAPKinase

Since p65 is a major component of NF-κB activated by LPS in macrophages, we evaluated the levels of p65 in nuclear extracts by western blotting analysis. Phosphorylation of IκB results in degradation and release of NF-κB, which then translocates to the nucleus. Therefore, we examined whether RFO could prevent phosphorylation of IκB induced by LPS treatment. Figure 3A shows that IκB phosphorylation was increased by treatment with LPS alone in cytosol level, but that such phosphorylation was significantly inhibited in the presence of RFO, similar to results

for the nuclear translocation of p65. Taken together, these data suggest that the inhibitory effect of RFO on the LPS-induced translocation of p65 might be involved in the suppression of IκB phosphorylation. To further investigate whether the inhibition of pro-inflammatory mediators by RFO is modulated through the MAPK pathway, we evaluated the effects of RFO on the LPS-induced phosphorylation of p38, ERK, and JNK (Figure 3B). RFO suppressed LPS-induced phosphorylation of p38, ERK and JNK. These results suggest that RFO blocks MAPK pathways to suppress the inflammatory response in LPS-induced RAW 264.7 macrophages.

Figure 3: Effect of RFO on the expression of NFκB, phosphor-IκB, and MAPK levels in LPS-induced RAW 264.7 cells.
The cells were incubated with 10-50 µg/mL of RFO in the presence or absence of LPS (1 µg/mL) for 24 h. The nucleus level of NFκB, the cytosol level of phospho-IκB expression (A), MAPK expression (B) in representative samples. The relative protein expression was densitometerically quantified using BioRad GS-670 densitometer and normalized to total MAPK proteins. The results from replication are expressed as the mean±S.D. (n=3). **p<0.05 and ***P<0.001 compared with the LPS group

HPLC analysis of RFO

Table 2 showed the HPLC analysis of RFO. HPLC revealed that 1 g of RFO had 14.05±0.8 mg of β-cryptoxanthin and 7.4 ± 0.7 mg of β-carotene.

Table 2: Component of RFO.

β-cryptoxanthin	14.05±0.8 mg/g
β-carotene	7.4±0.7 mg/g
Oleic acid	596.3 mg/g
Linoleic acid	70.1 mg/g
Linolenic acid	7.9 mg/g
Selenium	1.08 μg/g
α-tocopherol	132.3 mg/g
Total tocopherols	135 mg/g

Discussion

Inflammation is an immune response that protects our body against host response to infection and injury [19,20]. All inflammatory responses act through mononuclear cells, macrophages, and lymphocytes. Macrophages play on important innate immune effectors and increase pro-inflammatory factors including nitric oxide (NO), prostaglandin E_2 (PGE_2) cytokines.

The excessive amounts of NO and PGE_2 produced by activation of iNOS and COX-2 in response to LPS play an important role in inflammation [21,22]. The overproduction of iNOS-derived NO is involved in the pathology of various inflammatory disorders and tissue damage conditions. A change in the NO level through the inhibition of iNOS enzyme activity or iNOS induction provides a means of assessing the effect of these agents on the inflammatory process. iNOS is implicated in the synthesis of prostaglandin

H_2 starting of arachidonic acid, which is a precursor of PGE_2, in activated macrophages with LPS [23]. In addition, iNOS leads to overproduction of NO, PGE_2, and COX-2 which results in the production of inflammatory diseases. Thus, modulation of iNOS and NO expressions could be one of the strategies to reduce inflammatory diseases. The production of inflammatory cytokines is a crucial part of regulating inflammation and tumor progression. The key signaling pathway mediating the inflammatory response, the NF-κB transcription factor, has been well-established in various inflammatory diseases and cancers [24,25]. It is also well known that NF-κB is a significant role factor regulating the expression of inflammation-associated enzymes and cytokine genes, such as iNOS, COX-2, TNF-α and IL-1β, which contain NF-κB binding motifs within their respective promoters [1,26]. Therefore, this signaling pathway is a good target for anti-cancer and anti-inflammatory drug development. Many of the upstream kinases and downstream substrates are the same for the each of the major cascades. Our results revealed that anti-inflammatory activities of RFO are mediated through the inhibition of IκB phosphorylation and nuclear translocation of the NF-κB p65 subunit. Besides, these results also indicate that the inhibitory effects of RFO on MAPK and NF-κB signaling are related to a decrease in ROS. It is well known that oxidative stress stimulates ROS production in RAW 264.7 cell line [11,27]. Our data showed the pretreatment with RFO significantly decreased ROS production in LPS-induced RAW264.7 cells using DCFH-DA staining which demonstrated that RFO had a potent to reduce the oxidative stress. We also suggested that RFO regulated MAPK and NF-κB signaling of inflammation operate through oxidative stress. These results demonstrated that RFO could act as scavenging agents or acting on redox state of the cell and other acting as scavenging agents. In previous study, we already demonstrated that RFO regulated the cellular senescence through ROS modulation in H_2O_2-induced endothelial cells [5].

Carotenoids such as β-cryptoxanthin, β-carotene are one of the antioxidants which are not produced in the human body that must be ingested from outside. Many studies indicated that healthy people had the higher level of β-cryptoxanthin in blood [28-31]. β-cryptoxanthin is the only provitamin A component of carotenoid-based xanthophylls [14,32]. Carotenoids are lipid soluble components that must be ingested with fat to absorb completely in the body. Carotenoids affect the inflammation levels in blood as strong antioxidants and helps purify the blood. Park et al. showed that the daily oral administration of β-cryptoxanthin prevented the progression of osteoarthritis and inhibited proinflammatory cytokines in mice [33]. Therefore, we examined the effects of RFO on the production of several inflammatory mediators and on the expression levels of iNOS in LPS-induced RAW 264.7 macrophage cells. Our results demonstrated that RFO inhibited the expression of iNOS as well as the production of NO and PGE_2 and the mechanisms underlying the suppression of the inflammatory response of the NF-κB and ROS. According to the US USDA database, β-carotene content of RFO was significantly higher at 335 times of blackberry, 119 times of broccoli, 13.9 times of pumpkin, and 5.2 times for carrot [34,36]. In addition, β-cryptoxanthin content of RFO was significantly higher at 76 times of orange and 15 times of papaya [30,37]. These findings suggested that RFO might be a beneficial therapeutic agent in the treatment of a variety of inflammatory diseases.

Conclusion

RFO is Papuan traditional food and had been used to treat various disease for long time. In this study, we suggested RFO had an anti-inflammatory effect through regulating inflammatory mediators such as iNOS, COX-2, PGE_2, and excessive ROS for the first time. These physiological benefits of RFO may be attributed by regulation of NF-κB transcription. HPLC indicated that large number of carotenoids such as β-cryptoxanthin, β-carotene. This finding may be a synergistic adjuvant therapy for inflammatory diseases by acting as a radical scavenger, ROS inhibitor.

Acknowledgements

References

1. Rowley K, Walker KZ, Cohen J, Jenkins AJ, O'Neal D, et al. (2003) Inflammation and vascular endothelial activation in an Aboriginal population: relationships to coronary disease risk factors and nutritional markers. Med J Aust 178(10): 495-500.

2. Si Y, Guo S, Fang Y, Qin S, Li F, et al. (2015) Celery Seed Extract Blocks Peroxide Injury in Macrophages via Notch1/NF-kappaB Pathway. Am J Chin Med 43(3): 443-455.

3. Sahin K, Orhan C, Akdemir F, Tuzcu M, Sahin N, et al. (2017) β-Cryptoxanthin ameliorates metabolic risk factors by regulating NF-kappaB and Nrf2 pathways in insulin resistance induced by high-fat diet in rodents. Food Chem Toxicol 107(Pt A): 270-279.

4. Rhee YH, Rhee CH, Chung PS, Ahn JC (2017) Antioxidant and anti-inflammatory effects of rice bran and green tea fermentation mixture on lipopolysaccharideinduced RAW 264.7 macrophages. Tropical Journal of Pharmaceutical Research 16(12): 2943-2951.

5. Rhee YH, Mo JH, Kim JS (2019) Anti-senescence effect of Pandanus conoideus Lamk on ROS metabolism in human umbilical vein endothelial cells. BioCell 43(3):151-157.

6. Nuringtyas TR, Pratama Y, Wahyuono GS, Moeljopawiro S (2014) Cytotoxicity of Buah Merah (Pandanus conoideus Lamk.) Extract on Breast Cancer Cell Line (T47D). Inudroineinsigatny aJso uetr nalal of Biotechnology 19(1): 71-78.

7. Sugiritama IW, Dewi Ratnayanti IGA, Sri Wiryawan IGN, Ika Wahyuniari IA, Linawati NM, et al. (2016) Effect of Red Fruit Oil (Pandanus Conoideus Lam) on Animal Model of Preeclampsia. International Journal of Science and Research 5(7): 1770-1773.

8. Felle ZR, Wijayanti MA, Supargiyono (2013) The Effect of Pandanus conoideus Lamk Extract to the Serum Level of TNF-a, IL-10 and Parasitemia of Plasmodium berghei Infected in Mice. Tropical Medicine Journal 3(1): 39-47.

9. Sumarsono P, Widjiati, Susilowati S (2016) Red fruit oil increases trophoblast cells and decreases caspase-9 expression in placenta of lead exposed mice. Universa Medicina 35(2): 110-118.

10. Roreng MK, Palupi NS, Prangdimurti E (2014) Carotenoids from Red Fruit (Pandanus Conoideus Lam.) Extract Are Bioavailable: A Study in Rats. IOSR Journal of Pharmacy 4(2): 11-16.

11. Popkov VA, Fetisova AN, Nesterova OV, Samylina IA (2001) Experience in using phytopreparations to prevent and correct inflammatory urinary tract diseases. Vestn Ross Akad Med Nauk (2): 11-13.

12. Rohman A, Man YB, Riyanto S (2011) Authentication analysis of red fruit (Pandanus Conoideus Lam) oil using FTIR spectroscopy in combination with chemometrics. Phytochem Anal 22(5): 462-467.

13. Matsumoto C, Ashida N, Yokoyama S, Tominari T, Hirata M, et al. (2013) The protective effects of β-cryptoxanthin on inflammatory bone resorption in a mouse experimental model of periodontitis. Biosci Biotechnol Biochem 77(4): 860-862.

14. Gammone MA, Riccioni G, D'Orazio N (2015) Carotenoids: potential allies of cardiovascular health? Food Nutr Res 59: 26762.

15. Kobori M, Ni Y, Takahashi Y, Watanabe N, Sugiura M, et al (2014) **β**-Cryptoxanthin alleviates diet-induced nonalcoholic steatohepatitis by suppressing inflammatory gene expression in mice. PLoS One 9(5): e98294.

16. Tanaka T, Tanaka T, Tanaka M, Kuno T (2012) Cancer chemoprevention by citrus pulp and juices containing high amounts of β-cryptoxanthin and hesperidin. J Biomed Biotechnol 2012: 1-10.

17. Sarungallo ZL, Hariyadia P, Andarwulana N, Purnomoa EH, Wadad M (2015) Analysis of α-cryptoxanthin, β-cryptoxanthin, α -carotene, and β-carotene of Pandanus conoideus oil by high-performance liquid chromatography (HPLC). Procedia Food Science 3: 231-243.

18. Johnstone AM, Lobley GE, Horgan GW, Bremner DM, Fyfe CL, et al. (2011) Effects of a high-protein, low-carbohydrate v. high-protein, moderate-carbohydrate weight-loss diet on antioxidant status, endothelial markers and plasma indices of the cardiometabolic profile. Br J Nutr 106(2): 282-291.

19. Lin MH, Chen MC, Chen TH, Chang HY, Chou TC (2015) Magnolol ameliorates lipopolysaccharide-induced acute lung injury in rats through PPAR-gamma-dependent inhibition of NF-kB activation. Int Immunopharmacol 28(1): 270-278.

20. Thummuri D, Jeengar MK, Shrivastava S, Nemani H, Ramavat RN, et al. (2015) Thymoquinone prevents RANKL-induced osteoclastogenesis activation and osteolysis in an in vivo model of inflammation by suppressing NF-KB and MAPK Signalling. Pharmacol Res 99: 63-73.

21. Katsuura S, Imamura T, Bando N, Yamanishi R (2009) β-Carotene and β-cryptoxanthin but not lutein evoke redox and immune changes in RAW264 murine macrophages. Mol Nutr Food Res 53(11): 1396-1405.

22. Liu XR, Wang YY, Dan XG, Kumar A, Ye TZ, et al. (2016) Anti-inflammatory potential of β-cryptoxanthin against LPS-induced inflammation in mouse Sertoli cells. Reprod Toxicol 60: 148-155.

23. Khan MA, Khan MJ (2018) Nano-gold displayed anti-inflammatory property via NF-kB pathways by suppressing COX-2 activity. Artif Cells Nanomed Biotechnol 46(sup1): 1149-1158.

24. Kramer MS, Kahn SR, Platt RW, Genest J, Rozen R, et al (2009) Antioxidant vitamins, long-chain fatty acids, and spontaneous preterm birth. Epidemiology 20(5): 707-713.

25. Kerley CP (2019) Dietary patterns and components to prevent and treat heart failure: a comprehensive review of human studies. Nutr Res Rev 32(1): 1-27.

26. Zhang J, Dhakal IB, Lang NP, Kadlubar FF (2010) Polymorphisms in inflammatory genes, plasma antioxidants, and prostate cancer risk. Cancer Causes Control 21(9): 1437-1444.

27. Suzuki K, Ito Y, Ochiai J, Yasuhiro Kusuhara, Shuji Hashimoto, et al. (2003) Relationship between obesity and serum markers of oxidative stress and inflammation in Japanese. Asian Pac J Cancer Prev 4(3): 259-266.

28. Pattison DJ, Symmons DP, Lunt M, Welch A, Bingham SA, et al. (2005) Dietary β-cryptoxanthin and inflammatory polyarthritis: results from a population-based prospective study. Am J Clin Nutr 82(2): 451-455.

29. Karppi J, Kurl S, Makikallio TH, Ronkainen K, Laukkanen JA (2013) Low levels of plasma carotenoids are associated with an increased risk of atrial fibrillation. Eur J Epidemiol 28(1): 45-53.

30. Hirata N, Ichimaru R, Tominari T et al (2019) β -Cryptoxanthin Inhibits Lipopolysaccharide-Induced Osteoclast Differentiation and Bone Resorption via the Suppression of Inhibitor of NF-kappaB Kinase Activity. Nutrients 11(2).

31. Hikita M, Motojima K, Kamata S, Yoshida T, Tanaka-Nakadate S, et al. (2016) Protective Efficacy of the Ingestion of Mandarin Orange Containing β-Cryptoxanthin on Lipopolysaccharide-induced Acute Nephritis. Yakugaku Zasshi 136(7): 1031-1040.

32. Han X, Li W, Huang D, Yang X (2016) Polyphenols from hawthorn peels and fleshes differently mitigate dyslipidemia, inflammation and oxidative stress in association with modulation of liver injury in high fructose diet-fed mice. Chem Biol Interact 257: 132-140.

33. Park G, Horie T, Fukasawa K, Kakeru Ozaki, Yuki Onishi, et al (2017) Amelioration of the Development of Osteoarthritis by Daily Intake of β-Cryptoxanthin. Biol Pharm Bull 40(7): 1116-1120.

34. Amani R, Parohan M, Jomehzadeh N, Haghighizadeh MH (2019) Dietary and Biochemical Characteristics Associated with Normal-Weight Obesity. Int J Vitam Nutr Res: 1-6.

35. Philippou E, Nikiphorou E (2018) Are we really what we eat? Nutrition and its role in the onset of rheumatoid arthritis. Autoimmun Rev 17(11): 1074-1077.

36. Barros MP, Rodrigo MJ, Zacarias L (2018) Dietary Carotenoid Roles in Redox Homeostasis and Human Health. J Agric Food Chem 66(23): 5733-5740.

37. Toti E, Chen CO, Palmery M, Villano Valencia D, Peluso I (2018) Non-Provitamin A and Provitamin A Carotenoids as Immunomodulators: Recommended Dietary Allowance, Therapeutic Index, or Personalized Nutrition? Oxid Med Cell Longev 2018: 4637861.

Your next submission with Juniper Publishers will reach you the below assets

- Quality Editorial service
- Swift Peer Review
- Reprints availability
- E-prints Service
- Manuscript Podcast for convenient understanding
- Global attainment for your research
- Manuscript accessibility in different formats
  (Pdf, E-pub, Full Text, Audio)
- Unceasing customer service

Track the below URL for one-step submission
https://juniperpublishers.com/online-submission.php